Synthesis, structure, and characterization of hybrid materials: $[Ce(H_2O)]_2[O_2C(CH_2)_2CO_2]_3$ and $[Sm(H_2O)]_2[O_2C(CH_2)_2CO_2]_3 \cdot H_2O$

A. Seguatni,[a,b] M. Fakhfakh,[a,b] M.J. Vauley,[c] and N. Jouini[d,*]

[a] Laboratoire de Cristallochimie, Faculté des Sciences de Tunis, Campus Universitaire, Le Belvédère, Tunis 1060, Tunisia
[b] Laboratoire de Chimie Inorganique et Structurale, Faculté des Science de Bizerte, 7021 Zarzouna, Bizerte, Tunisia
[c] ITODYS, Unité associée CNRS 7086, Université Paris VII- Denis Diderot, Case 7090. 2, place Jussieu, 75251 Paris Cedex 05, France
[d] LPMTM.-UPR-CNRS 9001, Institut Galilée, Université Paris XIII. 99, avenue J.B. Clément, 93430 Villetaneuse, France

Abstract

The rare-earth dicarboxylate hybrid materials $[Ce(H_2O)]_2[O_2C(CH_2)_2CO_2]_3$ ([*Ce(Suc)*]) and $[Sm(H_2O)]_2[O_2C(CH_2)_2CO_2]_3 \cdot H_2O$ ([*Sm(Suc)*]) have been hydrothermally synthesized (200°C, 3 days) under autogenus pressure. [Ce(Suc)] is triclinic, $a = 7.961$ (3) Å, $b = 8.176$ (5) Å, $c = 14.32$ (2) Å, $\alpha = 97.07°$ (7), $\beta = 96.75°$ (8), $\gamma = 103.73°$ (6), and $z = 2$. The crystal structure of this compound has been determined using 3120 unique single crystal data. The final refinements let the agreement factors R_1 and $wR_2(F^2)$ converge to 0.0138 and 0.0363, respectively. [Ce(Suc)] is built up from infinite chains of edge-sharing nine-fold coordinated cerium atoms running along [100]. These chains are interconnected by the carbon atoms of the succinate anions, leading to a three-dimensional hybrid framework. The cell constants of [Sm(Suc)], isotypic with monoclinic $C2/c$ $[Pr(H_2O)]_2[O_2C(CH_2)_2CO_2]_3 \cdot H_2O$ ([Pr(Suc)]), were refined starting from X-ray powder data: $a = 20.275$ (3) Å, $b = 7.919$ (6) Å, $c = 14.130$ (3) Å, and $\beta = 121.45°$ (1). Despite its lower symmetry, [Ce(Suc)] presents an important structural filiation with [Sm(Suc)]
© 2004 Elsevier Inc. All rights reserved.

1. Introduction

Over the last few years, numerous works have been carried out using the hydrothermal route to prepare new opened structure materials. Several structural agents have been used in these syntheses, leading to various structural types. For instance, Haushalter et al.'s works on the newly isolated phospho-vanadate materials [1,2] can be quoted. In the same context, also in order to supplant the zeolyte-type materials by compounds with great pore sizes, Ferey et al. prepared some gallium and aluminum-templated phosphates [3–7].

Also using the hydrothermal method, the chemistry of hybrid materials have been widely developed. A metal cation and a bi-functional (multi-functional) organic molecule, such as diphosphonates or dicarboxylates, are involved in these types of compounds. The organic molecules act as spacers between inorganic parts to build materials with a porosity that depends on the shape of the organic molecule and the host structure of the whole hybrid material [8–12].

This research field is quite recent; however, the isolated compounds have already shown a rich crystal chemistry owing to the numerous structural types encountered [13]. The isolated porous hybrid materials can be successfully used either in water sorption and desorption [14] or in catalysis as substrates on which catalyzers can be deposited. They may also be used in various fields of applications such as magnetism, ferroelectricity, and optics, depending on the nature of the involved metal cation [15].

This paper relates a contribution to the study of rare-earth hybrid carboxylate materials that has already been initiated by G. Ferey et al. [16–19].

*Corresponding author. Fax: +0033-1-49-40-39 38.
E-mail address: jouini@lpmtm.univ-paris13.fr (N. Jouini).

2. Experimental

2.1. Preparations

The compound $[Ce(H_2O)]_2[O_2C(CH_2)_2CO_2]_3$, the formula of which was found by structural determination, is prepared using the hydrothermal method under autogenous pressure starting from cerium chloride heptahydrate: $CeCl_3 \cdot 7H_2O$; succinic acid: $HOOC(CH_2)_2COOH$; potassium hydroxide: KOH; and desionized water: H_2O in the molar ratio 1:2:1.5:450. First, cerium chloride and succinic acid are dissolved separately into a small amount of water, then potassium hydroxide is added to the acidic solution. The solutions are mixed, and the synthesis is performed in a Teflon-lined autoclave at 473 K for 3 days. The product contains parallelepipedic colorless crystals. The same method of preparation was carried out for the synthesis of $[Sm(H_2O)]_2[O_2C(CH_2)_2CO_2]_3 \cdot H_2O$. The starting materials $Sm(NO_3)_3 \cdot 7H_2O$, $HOOC(CH_2)_2COOH$, KOH, and H_2O were introduced in the molar ratio of 2:3:5:610. In both cases, the reaction product was filtered, washed with desionized water, and dried in air. Elemental analysis complies with the formula proposed. For [Ce(Suc)], the experimental/calculated H and C yields are 2.3/2.7% and 21.3/21.7%, respectively. These yields take the values of 2.3/2.4 and 20.1/20.5 for [Sm(Suc)].

2.2. X-ray powder diffraction study

The X-ray powder diffraction data of [Ce(Suc)] is in agreement with that calculated on the basis of the structural data (Fig. 1). The diffraction peaks of the [Sm(Suc)] X-ray diffraction pattern (Fig. 2) are very similar in intensity and positions to those appearing in
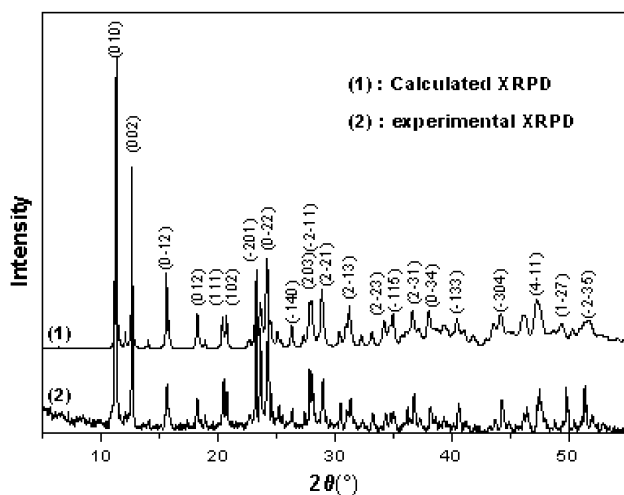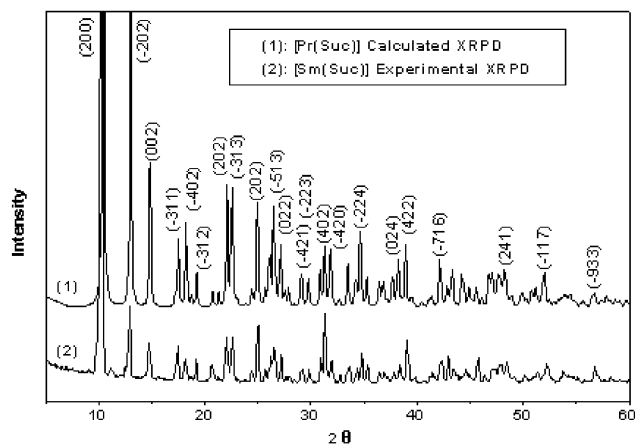

Fig. 2. Experimental X-ray powder diffraction diagram of: $[Sm(H_2O)]_2[O_2C(CH_2)_2CO_2]_3 \cdot H_2O$ compared to that of $[Pr(H_2O)]_2$ $[O_2C(CH_2)_2CO_2]_3 \cdot H_2O$ of G. Ferey.

the [Pr(Suc)] XRPD. The lattice constants refined starting from the X-ray powder data using the Powderx program[1] are very close, for [Ce(Suc)], to the values obtained by the fit of the 25 data collected on the single crystal. When these refinements were carried out on the samarium compound, the cell constants obtained were: $a = 20.275$ (3) Å, $b = 7.919$ (6) Å, $c = 14.130$ (4) Å, and $\beta = 121.45°(1)$.

2.3. Structure refinements

Data collection were performed on a parallelepipedic crystal of $[Ce(H_2O)]_2[O_2C(CH_2)_2CO_2]_3$. The preliminary Lorentz-polarization corrections and data analyses were carried out using the XCAD4 routine of the Wingx [20] integrated system of Windows programs. The absorption corrections were performed using the empirical Psi-scan method [21]. The structure solution was performed by the SHELXS 97 program using the Patterson method [22], which gave the cerium and oxygen atoms' positions. Subsequent refinements followed by Fourier syntheses allowed us to locate the carbon atoms. At this stage, the agreement factors R_1 and w$R_2(F^2)$ have already reached the following values of 0.0420 and 0.0996. These values decreased to 0.0191 and 0.0514, once the anisotropic thermal factors were refined. Then, the hydrogen atoms' positions were picked up from the Fourier map that showed peaks of about $1\,e\,Å^{-3}$ near the carbon and water molecule oxygen atoms. The final refinements made the agreement factors R_1 and w$R_2(F^2)$ decrease to the values of 0.0138 and 0.0363, respectively. The resulting Fourier map is featureless with maxima and minima ranging from 0.39 to $-0.43\,e\,Å^{-3}$, in the vicinity of a cerium atom. Note that no constraint was

Fig. 1. Experimental X-ray powder diffraction diagram of $[Ce(H_2O)]_2[O_2C(CH_2)_2CO_2]_3$ compared to the calculated one.

Table 1
Data collection conditions and refinements results

Equipment	CAD-4 Enraf Nonius Diffractometer
Wavelength	$\lambda(\mathrm{Mo}K\bar{\alpha}) = 0.70073$ Å
Chemical formula	$[\mathrm{Ce(OH)}]_2[\mathrm{C_4H_4O_4}]_3$
a (Å)	7.961 (3)
b (Å)	8.176 (5)
c (Å)	14.32 (2)
α (deg)	97.07 (7)
β (deg)	96.75 (8)
γ (deg)	103.73 (6)
$V(\text{Å}^3)$	888.09
z	2
Space group	$P\bar{1}$
ρ (g cm^{-3})	2.485
μ (mm^{-1})	5.14
Number of collected data	3259
Number of independent data	3120
Number of independent data with $I > 2\sigma(I)$	3011
$h\,k\,l$ limits for data collection	$-9 \leqslant h \leqslant 9$; $-9 \leqslant k \leqslant 9$; $0 \leqslant l \leqslant 16$
Scan mode	$\omega - 2\theta$
Scan width (deg)	$\delta = 0.80 + 0.35 \mathrm{tg}\,\theta$
Recording range (deg)	$2.0 < \theta < 25.0$
Periodically monitored reflections	$(\bar{6}40)(6\bar{3}0)(\bar{4}21)(6\bar{4}0)$
R(int)	0.0117
Absorption correction type	Empirical (Psi-scan)
Number of parameters during refinements	318
Number of restraints	16
$R_1/wR_2(F^2)$	0.0138/0.0363
R_1 for 3011 data with $I > 2\sigma(I)$	0.0134
Extinction parameter	6.42×10^{-3}

imposed upon the hydrogen atoms positions during refinements, but some restraints were applied to give reasonable distances and angles involving hydrogen atoms. The data collection conditions and the refinement results are gathered in Table 1. Table 2 presents atomic positions and isotropic or equivalent thermal factors. The anisotropic thermal factors of non-hydrogen atoms are reported in Table 3.

2.4. Infrared (IR) spectroscopy

The IR absorption spectra were carried out on the *PARAGON 1000 PC*, Perkin-Elmer FTIR spectrometer in the range 400–4000 cm^{-1} wave numbers, with five scans and 4.0 cm^{-1} increments on a pressed disc of each of the title compounds dispersed in KBr.

2.5. Thermal analysis

Thermal analysis was performed on a certain amount of a powdered sample of each of the title compounds using a SETARAM TG92 thermoanalyzer. The experi-

Table 2
Atomic coordinates and equivalent thermal parameters

Atom	x	y	z	$U_{\mathrm{iso}}/U_{\mathrm{eq}}$
Ce(1)	0.86959 (2)	−0.07116 (2)	0.71002 (1)	0.01409 (6)
Ce(2)	0.40896 (2)	0.01061 (2)	0.79730 (1)	0.01395 (6)
O(1w)	0.9991 (4)	−0.1731 (4)	0.5648 (2)	0.0401 (6)
H(11w)	0.983 (8)	−0.139 (8)	0.505 (3)	0.11 (3)*
H(12w)	1.118 (4)	−0.177 (9)	0.577 (5)	0.13 (3)*
O(2w)	0.6583 (3)	0.1882 (3)	0.9220 (2)	0.0263 (5)
H(21w)	0.764 (4)	0.162 (5)	0.919 (3)	0.05 (2)*
H(22w)	0.642 (7)	0.192 (7)	0.986 (2)	0.08 (2)*
O(1A)	0.8601 (3)	−0.3813 (3)	0.7240 (2)	0.0340 (6)
O(2A)	1.1188 (3)	−0.2044 (3)	0.7710 (2)	0.0219 (5)
C(1A)	1.0165 (4)	−0.3554 (4)	0.7587 (2)	0.0190 (6)
C(2A)	1.0878 (4)	−0.5015 (4)	0.7874 (3)	0.0237 (7)
H(21A)	1.173 (5)	−0.464 (6)	0.847 (2)	0.05 (2)*
H(22A)	0.994 (4)	−0.594 (4)	0.799 (3)	0.023 (8)*
C(3A)	0.1780 (5)	0.4293 (4)	0.7081 (3)	0.0270 (7)
H(31A)	0.096 (5)	0.386 (5)	0.649 (2)	0.04 (2)*
H(32A)	0.277 (5)	0.521 (5)	0.699 (4)	0.06 (2)*
C(4A)	0.2515 (4)	0.2859 (4)	0.7373 (2)	0.0209 (6)
O(3A)	0.3947 (3)	0.3188 (3)	0.7903 (2)	0.0339 (6)
O(4A)	0.1647 (3)	0.1295 (3)	0.7071 (2)	0.0228 (5)
O(1B)	0.4426 (3)	−0.2162 (3)	0.9017 (2)	0.0244 (5)
O(2B)	0.6562 (3)	−0.1559 (3)	0.8187 (2)	0.0213 (5)
C(1B)	0.5876 (4)	−0.2353 (4)	0.8822 (2)	0.0165 (6)
C(2B)	0.6765 (4)	−0.3548 (4)	0.9286 (3)	0.0213 (6)
H(21B)	0.667 (5)	−0.452 (4)	0.880 (2)	0.030 (9)*
H(22B)	0.603 (4)	−0.398 (4)	0.974 (2)	0.021 (8)*
C(3B)	1.1339 (4)	0.2737 (4)	1.0235 (2)	0.0196 (6)
H(31B)	1.067 (4)	0.218 (4)	1.069 (2)	0.029 (9)*
H(32B)	1.078 (4)	0.359 (4)	1.002 (3)	0.022 (8)*
C(4B)	1.1186 (4)	0.1462 (4)	0.9339 (2)	0.0172 (6)
O(3B)	1.2457 (3)	0.0841 (3)	0.9235 (2)	0.0269 (5)
O(4B)	0.9769 (3)	0.1090 (3)	0.8758 (2)	0.0253 (5)
O(1C)	0.8102 (3)	0.1344 (3)	0.5961 (2)	0.0339 (6)
O(2C)	0.6601 (3)	0.1297 (3)	0.7150 (2)	0.0201 (4)
C(1C)	0.6939 (4)	0.1809 (4)	0.6363 (2)	0.0184 (6)
C(2C)	0.5958 (4)	0.2993 (4)	0.5959 (2)	0.0194 (6)
H(21C)	0.605 (5)	0.393 (4)	0.647 (2)	0.03 (1)*
H(22C)	0.475 (3)	0.231 (4)	0.586 (3)	0.04 (1)*
C(3C)	0.3424 (4)	−0.3613 (4)	0.4944 (2)	0.0172 (6)
H(31C)	0.363 (4)	−0.472 (3)	0.499 (2)	0.013 (7)*
H(32C)	0.216 (3)	−0.379 (4)	0.491 (3)	0.021 (8)*
C(4C)	0.4391 (4)	−0.2419 (4)	0.5841 (2)	0.0173 (6)
O(3C)	0.6006 (3)	−0.2255 (3)	0.6027 (2)	0.0303 (5)
O(4C)	0.3543 (3)	−0.1647 (3)	0.6354 (2)	0.0302 (5)

Note: Only hydrogen atoms (*) are isotropically refined.

ment was carried out under air flow with a 5°C min^{-1} heating rate.

3. Description and discussion

The X-ray powder diffraction study reveals that $[\mathrm{Sm(H_2O)}]_2[\mathrm{O_2C(CH_2)_2CO_2}]_3 \cdot \mathrm{H_2O}$ is isotypic with $[\mathrm{Pr(H_2O)}]_2[\mathrm{O_2C(CH_2)_2CO_2}]_3 \cdot \mathrm{H_2O}$ [16]. Despite the lack

Table 3
Anisotropic thermal parameters of non-hydrogen atoms

Atoms	U_{11}	U_{22}	U_{33}	U_{23}	U_{13}	U_{12}
Ce(1)	0.01163 (9)	0.01701 (9)	0.01502 (9)	0.00222(6)	0.00188(6)	0.00658 (6)
Ce(2)	0.01150 (9)	0.01553 (9)	0.01565 (9)	0.00068(6)	0.00213(6)	0.00594 (6)
O(1w)	0.035 (2)	0.055 (2)	0.030 (2)	−0.003 (2)	0.014 (2)	0.013 (2)
O(2w)	0.021 (2)	0.037 (2)	0.020 (2)	−0.0020 (9)	0.0010 (9)	0.0090 (9)
O(1A)	0.021 (2)	0.019 (2)	0.058 (2)	0.003 (1)	−0.006 (1)	0.0046 (9)
O(2A)	0.018 (1)	0.018 (1)	0.030 (2)	0.0054 (8)	−0.0003 (8)	0.0049 (8)
C(1A)	0.020 (2)	0.018 (2)	0.019 (2)	−0.001 (2)	0.006 (2)	0.006 (2)
C(2A)	0.025 (2)	0.019 (2)	0.030 (2)	0.007 (2)	0.005 (2)	0.009 (2)
C(3A)	0.035 (2)	0.021 (2)	0.030 (2)	0.006 (2)	0.009 (2)	0.015 (2)
C(4A)	0.024 (2)	0.019 (2)	0.024 (2)	0.005 (2)	0.009 (2)	0.010 (2)
O(3A)	0.025 (2)	0.021 (2)	0.052 (2)	−0.001 (1)	−0.007 (2)	0.0066 (9)
O(4A)	0.021 (1)	0.017 (1)	0.031 (2)	0.0041 (9)	0.0040 (9)	0.0059 (8)
O(1B)	0.018 (1)	0.035 (2)	0.023 (2)	0.0094 (9)	0.0058 (8)	0.0087 (9)
O(2B)	0.022 (1)	0.024 (1)	0.022 (1)	0.0085 (9)	0.064 (8)	0.0090 (9)
C(1B)	0.016 (2)	0.015 (2)	0.015 (2)	−0.001 (1)	0.001 (1)	0.001 (2)
C(2B)	0.022 (2)	0.017 (2)	0.023 (2)	0.004 (2)	−0.002 (2)	0.003 (2)
C(3B)	0.019 (2)	0.021 (2)	0.019 (2)	0.001 (2)	0.001 (2)	0.010 (2)
C(4B)	0.017 (2)	0.019 (2)	0.016 (2)	0.005 (2)	0.005 (2)	0.004 (2)
O(3B)	0.021 (2)	0.038 (2)	0.023 (2)	−0.0048 (9)	0.0034 (9)	0.014 (1)
O(4B)	0.018 (1)	0.033 (2)	0.022 (2)	−0.0032 (9)	−0.0011 (8)	0.0049 (9)
O(1C)	0.038 (2)	0.050 (2)	0.033 (2)	0.025 (2)	0.021 (1)	0.032 (2)
O(2C)	0.022 (1)	0.022 (1)	0.020 (1)	0.0063 (8)	0.0058 (8)	0.0081 (8)
C(1C)	0.016 (2)	0.020 (2)	0.017 (2)	0.003 (2)	0.001 (2)	0.003 (2)
C(2C)	0.020 (2)	0.023 (2)	0.016 (2)	0.000 (2)	0.002 (2)	0.010 (2)
C(3C)	0.018 (2)	0.015 (2)	0.019 (2)	0.002 (2)	0.001 (2)	0.005 (2)
C(4C)	0.018 (2)	0.019 (2)	0.016 (2)	0.005 (2)	0.002 (2)	0.006 (2)
O(3C)	0.020 (2)	0.038 (2)	0.029 (2)	−0.010 (1)	−0.0056 (9)	0.012 (1)
O(4C)	0.024 (2)	0.039 (2)	0.025 (2)	−0.010 (1)	0.0039 (9)	0.009 (1)
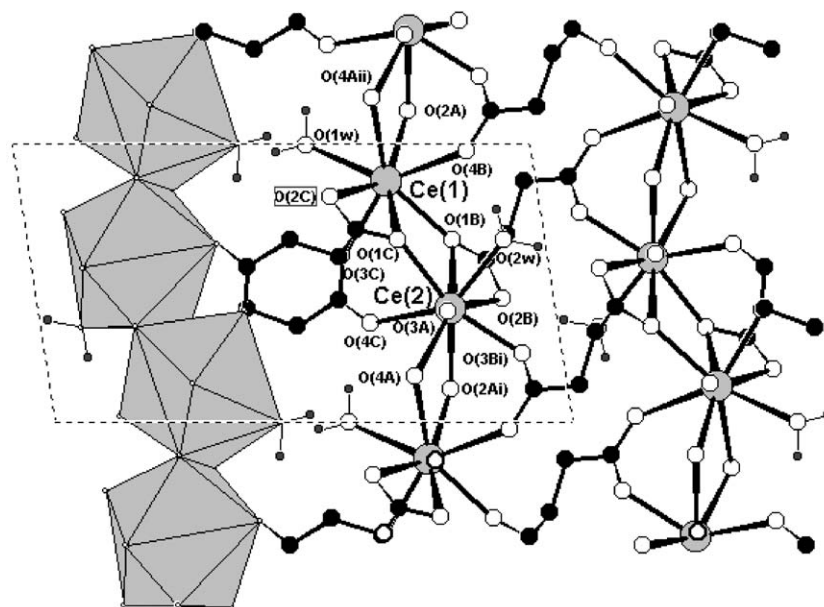
Fig. 3. The [010] view of the structure of $[Ce(H_2O)]_2[O_2C(CH_2)_2CO_2]_3$ showing the infinite $[Ce_2(H_2O)_2O_{12}]_n$ inorganic chains running along the [100] direction. Dotted lines indicate hydrogen bonds.

of hydration water, the $[Ce(H_2O)]_2[O_2C(CH_2)_2CO_2]_3$ hybrid compound presents important structural filiations with the hydrated praseodymium and samarium homologues. The [Ce(Suc)] inorganic network is built up of edge-sharing nine-fold coordinated $CeO_8(H_2O)$ polyhedra, leading to infinite $[Ce_2O_{12}(H_2O)_2]_n$ chains

running along the [100] direction (Fig. 3). In the praseodymium compound, the analogous inorganic chains are parallel to the [010] direction. In both the cerium and praseodymium compounds, these chains are interconnected by the carbon atoms of the succinate anions, leading to a three-dimensional hybrid framework.

The organic moiety of [Ce(Suc)] is composed of succinate anions (*A*, *B*, *C*) of three *crystallographically non-equivalent positions*. The carbon atoms of the A-type succinates are settled almost in the same plane that forms 83.0 and 81.5 dihedral angles with the carboxylate groups involving O(1A), O(2A), C(1A) and O(3A), O(4A), C(4A), respectively. On the contrary, the carbon atoms of the B and C succinates are not planar, they exhibit torsion angles of 70° and 88°, respectively.

In [Pr(Suc)], only two crystallographically independent succinate anions are observed. The carboxylates with carbon atoms settled in the same plane, like those of the A type in [Ce(Suc)], are less abundant. They present two pairs of crystallographically equivalent carbon atoms and two pairs of equivalent oxygen atoms. The succinates of the abundant type, where carbon atoms have independent positions, exhibit a dihedral angle of 72.5°, their homologues in [Ce(Suc)] being B and C succinates.

In [Ce(Suc)], the B and C type act almost in the [001] direction. Their homologues in [Pr(Suc)] also act nearly along the [001] direction. The main difference between the two structures resides in the role played by the remaining succinate anions. In [Ce(Suc)], the A-type succinate ensures the connection between the inorganic chains along the [010] direction (Fig. 4a), conferring to the [Ce(Suc)] hybrid material its three-dimensional character. Their homologues in [Pr(Suc)] present an angle of about 38° with the [100] direction (Fig. 4b). Taking into account this difference and the periodicity of two inorganic chains along the *a*-direction in [Pr(Suc)], instead of one inorganic chain along the *b*-direction in [Ce(Suc)], the *b* cell constant of Ce compound (8.17 Å) is close to the value obtained from the *a* cell constant of [Pr(Suc)] (20.26 Å) by the equation $2 \times b = a \cos(38)$.

Two of the six carboxylate groups encountered in [Ce(Suc] are strictly bridging. These groups involve the {C(4B), O(3B), O(4B)} and {C(4C), O(3C), O(4C)} atoms (Fig. 5). Similar behavior was encountered for one of the carboxylate functions of the most abundant bifunctional molecules in [Pr(Suc)]. The bridged polyhedra in both Ce and Pr compounds by such carboxylate groups are immediate neighbors of the same inorganic chain. The remaining carboxylate groups either have bridging or chelating function. In these carboxylate groups, the averages of the O···O distances and O–C–O angles are 2.193 (4) Å and 119.7° (3), respectively (Table 4). In the strictly bridging carbox-
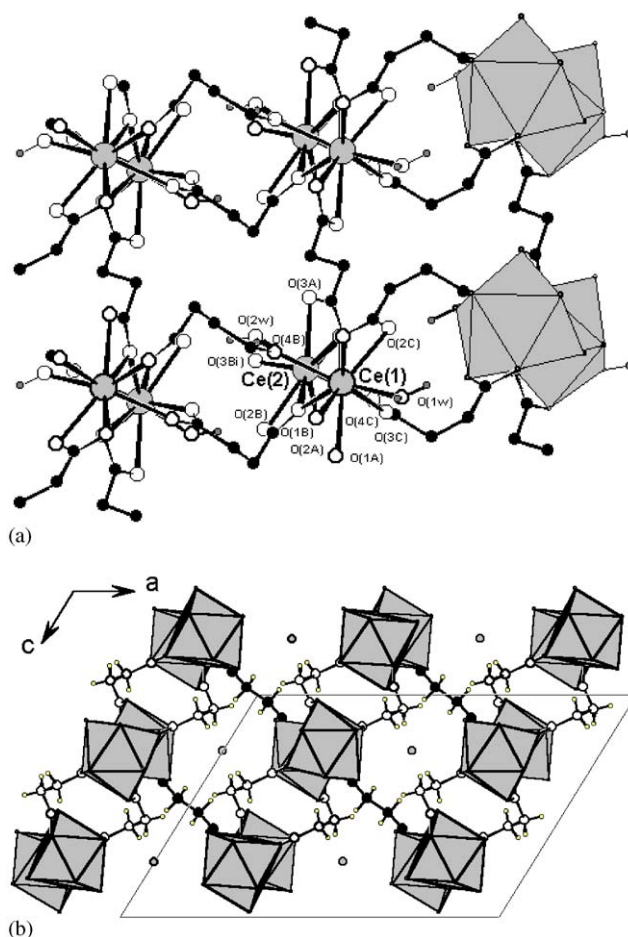

Fig. 4. (a) The [100] view of the structure of [Ce(H$_2$O)]$_2$[O$_2$C(CH$_2$)$_2$CO$_2$]$_3$ showing the connection between inorganic chains. Dotted lines indicate hydrogen bonds. (b) The [010] view of the structure of [Pr(H$_2$O)]$_2$[O$_2$C(CH$_2$)$_2$CO$_2$]$_3$·H$_2$O, showing the mode of connection between the succinate anions and the inorganic chains.
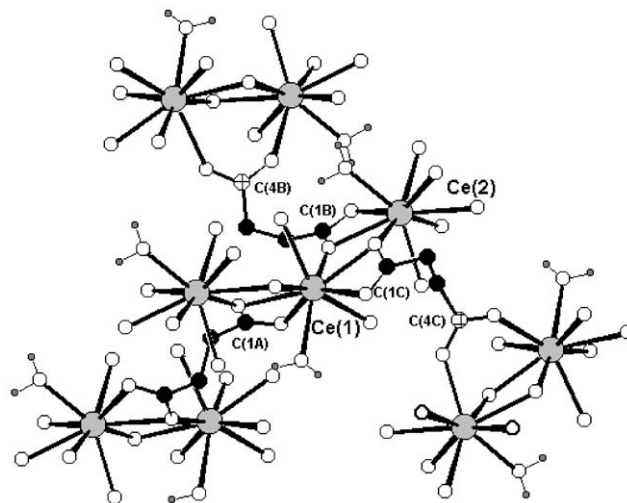

Fig. 5. A view of a fragment of the structure showing the mode of connection of the carboxylate groups (carbon atoms of the strictly bridging carboxylates are hatched).

Table 4
Main inter-atomic distances and polyhedral coordination angles Ce(1)O$_9$

Ce(1)	O(3C)	O(2B)	O(4Aii)	O(1A)	O(1w)	O(1C)	O(4B)	O(2A)	O(2C)
Ce(1)O$_9$									
O(3C)	2.451 (4)	76.1 (2)	140.4 (1)	77.7 (1)	79.9 (2)	74.5 (2)	141.6 (1)	125.2 (1)	74.0 (1)
O(2B)	3.035 (6)	2.473 (3)	141.5 (1)	74.2 (1)	145.1 (1)	118.2 (1)	69.8 (2)	101.4 (1)	70.0 (1)
O(4Aii)	4.690 (5)	4.727 (5)	2.535 (3)	117.7 (1)	70.2 (1)	74.4 (1)	71.7 (2)	69.9 (1)	103.4 (1)
O(1A)	3.140 (4)	3.032 (4)	4.354 (5)	2.552 (3)	76.2 (2)	145.0 (1)	108.5 (1)	50.4 (1)	138.5 (1)
O(1w)	3.219 (4)	4.804 (6)	2.931 (5)	3.157 (5)	2.562 (4)	78.2 (2)	138.5 (1)	72.6 (2)	126.4 (1)
O(1C)	3.038 (4)	4.324 (6)	3.084 (4)	4.880 (5)	3.234 (4)	2.566 (3)	106.5 (2)	139.7 (1)	50.2 (1)
O(4B)	4.740 (7)	2.886 (4)	2.988 (5)	4.156 (5)	4.799 (7)	4.115 (7)	2.569 (4)	79.5 (1)	78.1 (1)
O(2A)	4.481 (5)	3.924 (4)	2.940 (4)	2.192 (4)	3.055 (6)	4.846 (5)	3.304 (4)	2.596 (3)	157.6 (1)
O(2C)	3.043 (4)	2.914 (4)	4.033 (3)	4.822 (4)	4.611 (5)	2.191 (4)	3.260 (5)	5.102 (4)	2.605 (3)

Ce(2)	O(3Bi)	O(2C)	O(4C)	O(2Ai)	O(2w)	O(3A)	O(1B)	O(4A)	O(2B)
Ce(2)O$_9$									
O(3Bi)	2.443 (4)	142.8 (1)	139.3 (1)	71.9 (1)	80.0 (1)	74.0 (1)	79.9 (1)	77.1 (1)	123.8 (1)
O(2C)	4.684 (6)	2.499 (3)	73.3 (2)	142.4 (1)	71.7 (2)	75.9 (1)	117.7 (1)	99.6 (1)	68.8 (1)
O(4C)	4.637 (7)	2.985 (4)	2.503 (4)	69.3 (2)	140.7 (1)	112.4 (1)	100.3 (2)	78.3 (1)	80.2 (1)
O(2Ai)	2.904 (5)	4.737 (5)	2.848 (4)	2.505 (3)	144.5 (1)	115.2 (1)	73.5 (1)	69.5 (1)	107.7 (1)
O(2w)	3.195 (4)	2.946 (5)	4.738 (7)	4.795 (6)	2.529 (4)	75.6 (1)	80.9 (1)	124.8 (1)	70.9 (1)
O(3A)	3.013 (5)	3.114 (4)	4.209 (5)	4.279 (5)	3.119 (4)	2.563 (3)	147.3 (1)	50.0 (1)	137.1 (1)
O(1B)	3.215 (4)	4.333 (5)	3.888 (6)	3.031 (4)	3.303 (4)	4.918 (5)	2.563 (3)	140.9 (1)	49.4 (1)
O(4A)	3.175 (6)	3.931 (3)	3.254 (4)	2.940 (4)	4.587 (6)	2.204 (4)	4.910 (5)	2.647 (3)	157.8 (1)
O(2B)	4.500 (4)	2.914 (4)	3.326 (5)	4.168 (4)	3.008 (4)	4.857 (4)	2.184 (4)	5.205 (4)	2.656 (3)

C(1A)	O(1A)	O(2A)	C(2A)	C(4A)	O(3A)	O(4A)	C(3A)
Succinates							
O(1A)	1.243 (4)	120.2 (3)	120.3 (3)	O(3A)	1.245 (4)	120.5 (3)	119.9 (3)
O(2A)	2.192 (4)	1.286 (4)	119.5 (3)	O(4A)	2.204 (4)	1.294 (4)	119.7 (3)
C(2A)	2.399 (4)	2.426 (4)	1.518 (4)	C(3A)	2.388 (5)	2.427 (4)	1.510 (4)
C(1B)	O(1B)	O(2B)	C(2B)	C(4B)	O(3Bii)	O(4B)	C(3B)
O(1B)	1.259 (4)	118.7 (3)	121.4 (3)	O(3Bii)	1.251 (4)	124.7 (3)	117.7 (3)
O(2B)	2.184 (4)	1.280 (4)	119.9 (3)	O(4B)	2.233 (3)	1.270 (4)	117.6 (6)
C(2B)	2.417 (4)	2.417 (4)	1.509 (4)	C(3B)	2.379 (4)	2.393 (5)	1.524 (5)
C(1C)	O(1C)	O(2C)	C(2C)	C(4C)	O(3C)	O(4C)	C(3C)
O(1C)	1.253 (4)	119.3 (3)	121.6 (3)	O(3C)	1.253 (4)	123.8 (3)	117.2 (3)
O(2C)	2.191 (4)	1.286 (4)	119.0 (3)	O(4C)	2.221 (3)	1.265 (4)	119.0 (3)
C(2C)	2.414 (4)	2.410 (4)	1.507 (4)	C(3C)	2.368 (5)	2.399 (5)	1.515 (5)

(D) donor	H	(A) acceptor	D−H	H···A	D···A	D–H···A
Hydrogen bonds						
O(1w)	H(w11)	O(1C^{iii})	0.94 (4)	2.31 (5)	2.913 (5)	121 (5)
O(2w)	H(w21)	O(4B)	0.92 (3)	1.99 (3)	2.891 (5)	165 (4)
O(1w)	H(w12)	O(4C^{i})	0.95 (4)	1.94 (5)	2.871 (5)	165 (5)
O(2w)	H(w22)	O(1B^{iv})	0.94 (3)	1.82 (3)	2.737 (5)	164 (4)

(i) $x - 1, y, z$; (ii) $x + 1, y, z$; (iii) $-x, -y, 1 - z$; and (iv) $1 - x, -y, -z$.

ylate groups these averages are superior, the values encountered being 2.227 (3) Å and 124.3° (3), respectively.

The difference in the C–O distances is more pronounced for the carboxylate groups playing either bridging or chelating roles, in comparison with the strictly bridging ones. Indeed, the average of the shortest/longest C–O distances are 1.250 (4)/1.287 (4) Å, and 1.252 (4)/1.268 (4) Å for carboxylate groups of double character and strictly bridging, respectively.

Concerning the cerium coordination polyhedra, one can notice that the smallest O···O distances and O–Ce–O angles involve oxygen atoms of chelating carboxylate groups (Table 4). Indeed, the O–Ce–O average values involving such oxygen atoms are 50.3°(1) and 49.7°(1) for Ce(1) and Ce(2), respectively. These
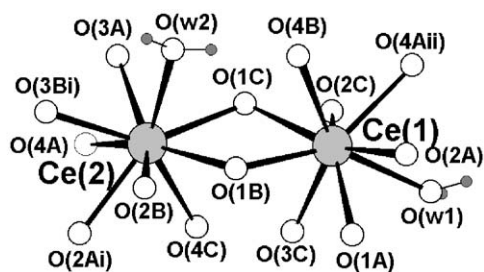
Fig. 6. The Ce(1) and Ce(2) environments.

Fig. 7. The $[Ce(H_2O)]_2[O_2C(CH_2)_2CO_2]_3$ and $[Sm(H_2O)]_2[O_2C(CH_2)_2CO_2]_3 \cdot H_2O$ IR spectra.

small values may explain the important distortion of the Ce coordination polyhedra.

Each cerium atom is coordinated to a water molecule oxygen atom, four oxygen atoms of a chelating group, two oxygen atoms of strictly bridging carboxylate groups, and two bridging oxygen atoms of carboxylate groups with a double character (Fig. 6). The same type of coordination is encountered for Pr in $[Pr(H_2O)]_2[O_2C(CH_2)_2CO_2]_3 \cdot H_2O$.

The hydrogen bonds presented in Figs. 3 and 4a in dotted lines are of two types. Those occurring between atoms belonging to the same inorganic chains, involve H(11w) and O(2C) atoms. Those acting between adjacent inorganic chains are stronger and oriented along either the *a*- or *c*-directions. The strong character of the "inter-chain" hydrogen bonds may play an important role on the whole structure packing.

Bond valence calculations [23] for Ce(1) and Ce(2) gave the values 3.13 and 3.15 v.u., respectively. These values are in agreement with trivalent cerium, as expected for an electro-neutral formula.

Either [Ce(Suc)] or [Pr(Suc)] present important structural filiations with $[Nd(H_2O)]_2[O_2C(CH_2)_3CO_2]_3 \cdot 4H_2O$ [17] and $[La_2(H_2O)_4(O_2C(CH_2)_3CO_2)_3] \cdot 6H_2O$ [24] that exhibit the same topology to be built up of infinite inorganic chains of nine-fold coordinated lanthanide polyhedra-sharing edges and di-carboxylates with an aliphatic carbon chain acting as linkers.

It was noticed that the tunnels these materials present are as large as the carbon chain of the carboxylate molecule is long, therefore, accommodating more hydration water molecules, [16].

If we keep the hypothesis that the cerium compound results from a triclinic distortion of its praseodymium homologue, we should admit such distortion results in the shrinkage of the tunnels and lack of hydration water in the cerium compound.

It is noteworthy that the topology adopted by some recently isolated europium hybrid compounds is different. The inorganic moiety of these materials comprises layers of nine coordinated europium polyhedra-sharing faces and/or edges pillared by benzene dicarboxylate [25].
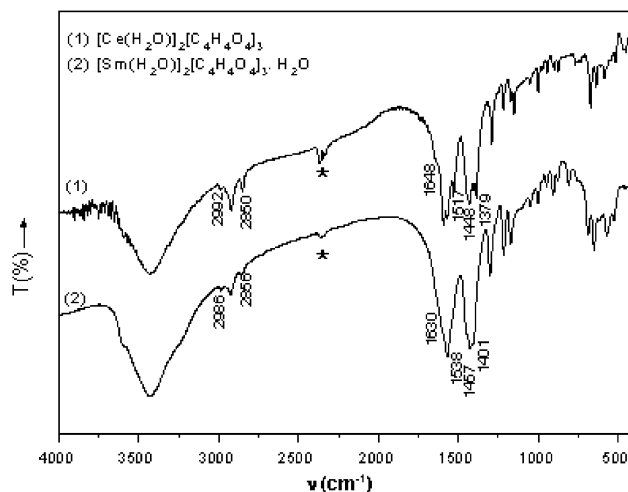
4. IR spectroscopy

IR characterization corroborates great structural filiations between the cerium and samarium compounds, which have already been shown by the X-ray powder diffraction study.

The IR spectra of [Ce(Suc)] and [Sm(Suc)] (Fig. 7), show three characteristic spectral regions of hybrid materials:

- Peaks appearing in the spectral range from 1379 to 1648 cm^{-1} for [Ce(Suc)] and from 1401 to 1630 for [Sm(Suc)] should be assigned to ν_s(C–O) and ν_{as}(C–O) of carboxylate groups, in addition to the δ(H–O–H) bending mode of the water molecules expected in the upper frequency range of this region.
- The spectral range from 2907 to 2992 cm^{-1} for [Ce(Suc)] and from 2911 to 2986 for [Sm(Suc)] is characteristic of the ν(C–H) vibrational modes of –CH$_2$– groups within the carbon chain.
- The upper range is reserved to ν(O–H) vibrational modes involving either the hydration of water molecules or those coordinated to the metal cation.

These assignment attempts are based on previous results encountered in the literature [26–29].

Note that the starred peaks in the region of about 2350 cm^{-1} correspond to atmospheric CO_2.

5. Thermal analysis

The thermal analysis results are in agreement with the structural data for both the cerium and samarium compounds.

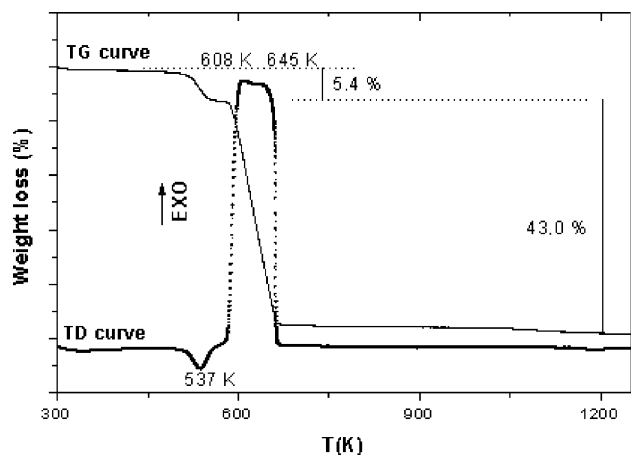The TD curve of [Ce(Suc)] shows two thermal phenomena, each accompanied by a weight loss

Fig. 8. The TG and TD curves of the $[Ce(H_2O)]_2[O_2C(CH_2)_2CO_2]_3$ material.

Fig. 9. The TG and TD curves of the $[Sm(H_2O)]_2[O_2C(CH_2)_2CO_2]_3 \cdot H_2O$ material.

(Fig. 8). The first thermal effect is endothermic; it occurs at 537 K and corresponds to the loss of only water molecule present in the compound and coordinated to the cerium. The experimental and theoretical weight losses are 5.4% and 5.40%, respectively. The second thermal effect is exothermic, it takes place from 608 to 645 K and corresponds to the combustion of the whole organic moiety (three organic molecules). Note that the X-ray powder diagram of the residue of thermal analysis experiment, annealed at 1200 K, shows this product to be CeO_2. The weight loss calculation done on the basis of CeO_2 as a residue is in agreement with the experimental value. Indeed, the experimental and the theoretical losses are 43.0% and 42.8%, respectively.

The TD curve of [Sm(Suc)] shows three thermal effects (Fig. 9). The first one at 487 K includes either hydration or crystallization water (experimental/theoretical weigh loss: 7.6/7.7%). The second thermal effect occurs at 730 K and it is accompanied by a weight loss of about two-thirds of the organic moiety (experimental/theoretical weigh loss: 34.1/33.0%) and should be attributed to the removal of the most abundant succinate anions (B and C). The third one, occurring at a much higher temperature (850 K), corresponds to the less abundant succinate (A), which seems more tightly bonded to the inorganic chains. The experimental weight loss value corresponding to whole organic moiety (42.7%) is in agreement with the calculated one (42.7%) when the thermal analysis residue is Sm_2O_3, which have been verified by XRPD after annealing for several hours at 1200 K.

6. Conclusion

Two hybrid materials have been hydrothermally prepared. The triclinic $P\bar{1}$ $[Ce(H_2O)]_2[O_2C(CH_2)_2CO_2]_3$

presents important structural filiations with the monoclinic $C2/c$ $[Pr(H_2O)]_2[O_2C(CH_2)_2CO_2]_3 \cdot H_2O$ material to which $[Sm(H_2O)]_2[O_2C(CH_2)_2CO_2]_3 \cdot H_2O$ [Sm(Suc)] is isostructural too. The networks of these materials present the same topology built up of infinite inorganic chains of polyhedra interconnected by the carbon atoms of bi-functional organic molecules, which confer to this type of material its three-dimensional character.

The IR spectroscopy, thermal study, and elemental microanalysis results are mainly in agreement with the structural data.

References

[1] V. Soghomonian, R.C. Haushalter, J. Zubieta, C.J. O'Connor, Inorg. Chem. 35 (1998) 2826.

[2] Y. Lu, R.C. Haushalter, J. Zubieta, Inorg. Chim. Acta 268 (1998) 257.

[3] F. Serpaggi, T. Loiseau, G. Férey, Acta. Crystallogr. C-53 (1997) 1568.

[4] N. Simon, N. Guillou, T. Loiseau, F. Taulle, G. Férey, J. Solid State Chem. 147 (1999) 92.

[5] C. Paulet, T. Loiseau, G. Férey, J. Mater. Chem. 10 (5) (2000) 1225.

[6] N. Simon, T. Loiseau, G. Férey, Solid State Sci. 1 (1999) 339.

[7] T. Loiseau, G. Férey, Microporous Mesoporous Mater. 609 (2000) 35–36.

[8] M. Riou-Cavellec, C. Albinet, J.M. Grenèche, G. Ferey, J. Mater. Chem. 11 (2001) 3166–3171.

[9] O.K. Barthelet, C. Merlier, C. Serre, M. Riou-Cavellec, D. Riou, G. Ferey, J. Mater. Chem. 12 (2002) 1132–1137.

[10] H. Li, M. Eddaoudi, M. O'Keeffe, O.M. Yaghi, Nature 402 (1999) 276.

[11] M. Daoudi, J. Kim, M. O'Keeffe, O.M. Yaghi, J. Am. Chem. Soc. 124 (2002) 376.

[12] M. Daoudi, J. Kim, J.B. Wachter, H.K. Chae, M. O'Keeffe, O.M. Yaghi, J. Am. Chem. Soc. 123 (2001) 4368–4369.

[13] G. Férey, Chem. Mater. 13 (2001) 3080.

[14] T.M. Reineke, M. Eddaoudi, M. Fehr, D. Kelly, O.M. Yaghi, J. Am. Chem. Soc. 121 (1999) 1651.

[15] G. Ferey, J. Solid State Chem. 153 (2000) 37.

[16] F. Serpaggi, G. Férey, Microporous Mesoporous Mater. 32 (1999) 311–318.

[17] F. Serpaggi, G. Férey, J. Mater. Chem. 8 (1998) 2737.

[18] C. Serre, G. Ferey, J. Mater. Chem. 12 (2002) 3053–3057.

[19] E. Antic-Fidancev, F. Serpaggi, G. Férey, J. Alloys Compd. 340 (2002) 88.

[20] L.J. Farrugia, J. Appl. Crystallogr. 32 (1999) 467.

[21] A.C.T. North, D.C. Phillips, F.S. Mathews, Acta Crystallogr. Sect. A 24 (1968) 351.

[22] G.M. Sheldrick, Z. Dauter, K.S. Wilson, H. Hope, L.C. Sieker, Acta Crystallogr. D-49 (1993) 18.

[23] N.E. Breese, M. O'Keeffe, Acta Crystallogr. Sect. B. 47 (1991) 192.

[24] V. Kiritsis, A. Michaelides, S. Skoulika, S. Golhen, L. Ouaheb, Inorg. Chem. 37 (1998) 3407.

[25] C. Serre, F. Millange, J. Marrot, G. Ferey, Chem. Mater. 14 (2002) 2409–2415.

[26] K. Nakamoto, in: Infrared and Raman Spectra of Inorganic and Coordination Compounds, 4th Edition, Wiley, New York, 1986.

[27] C. Livage, C. Egger, G. Férey, Chem. Mater. 11 (1999) 1546.

[28] C. Hornick, P. Rabu, M. Drillon, Polyhedron 19 (2000) 259.

[29] V. Laget, C. Hornick, P. Rabu, M. Drillon, J. Mater. Chem. 9 (1999) 169.